NOTES AND CORRESPONDENCE

EOF Representations of the Madden–Julian Oscillation and Its Connection with ENSO*

WILLIAM S. KESSLER

NOAA/Pacific Marine Environmental Laboratory, Seattle, Washington

28 March 2000 and 21 February 2001

ABSTRACT

Although recent El Niño events have seen the occurrence of strong intraseasonal winds apparently associated with the Madden–Julian oscillation (MJO), the usual indices of interannual variability of the MJO are uncorrelated with measures of the ENSO cycle. An EOF decomposition of intraseasonal outgoing longwave radiation and zonal wind identifies two modes of interannual variability of the MJO: a zonally stationary variation of amplitude that is unrelated to ENSO and a roughly 20°-longitude eastward extension of the MJO envelope during El Niño events. The stationary mode is represented by the first two EOFs, which form the familiar lag-correlated quadrature pair, and the eastward-extending mode is represented by the third EOF, which is usually ignored although it is statistically significant. However, the third EOF also has a systematic phase relation with the first pair, and all three should be considered as a triplet; rotating the EOFs makes the phase relation clear. The zonal shift represents about 20% of total MJO variance (which itself is about 55% of intraseasonal variance over the tropical strip). Although the eastward shift is small when compared with the global scale of the MJO, it produces a large proportional shift of MJO activity over the open Pacific, where physical interactions with ENSO processes can occur.

1. Introduction

The regular occurrence of strong intraseasonal oscillations over the western Pacific during the onset of El Niño events (Luther et al. 1983; Gutzler 1991; Kessler and McPhaden 1995; Verbickas 1998; McPhaden 1999) has sparked interest in the possibility of a physical connection between the two frequencies (Lau and Chan 1988; Weickmann 1991; Kessler et al. 1995; Fink and Speth 1997; Moore and Kleeman 1999; Slingo et al. 1999; Hendon et al. 1999; McPhaden and Yu 1999; Kessler and Kleeman 2000). Nevertheless, demonstrating such a connection has been controversial because indices of the most prominent intraseasonal signal, the Madden–Julian oscillation (MJO; Madden and Julian 1994) suggest that interannual changes in overall MJO activity are not related to the ENSO cycle (Slingo et al. 1999; Hendon et al. 1999). This has been taken as evidence that the MJO and the ENSO cycle do not interact in any substantive way.

Spatially coherent propagation across a wide zonal band distinguishes the MJO from the larger universe of intraseasonal variability, some of which is of small scale or otherwise unrelated; Hendon et al. (1999) estimated that only about one-half the intraseasonal variance over the west Pacific is associated with the MJO. A common method of extracting the coherent MJO signal has been based on the largest eigenvectors of bandpassed variability (Lau and Chan 1988; Zhang and Hendon 1997; Maloney and Hartmann 1998; among many others). Typically, a field, which could be tropical zonal wind at various levels or outgoing longwave radiation (OLR; a measure of tropical deep convection), is bandpassed to intraseasonal frequencies (periods of roughly 30–90 days) then decomposed in empirical orthogonal functions (EOFs) of some kind. The first two EOF modes generally appear as a quadrature pair that demonstrates a large-scale eastward-propagating intraseasonal signal. The temporal coefficients of this EOF pair can be used to create a low-frequency index of MJO activity (Slingo et al. 1999; Hendon et al. 1999; Jones 2000) or to construct a ''composite event'' (Shinoda et al. 1998; Maloney and Hartmann 1998). This general technique is robust in the sense that it is not particularly dependent on the variable studied, the details of the bandpass, or the type of EOF analysis employed. Such an analysis

* Pacific Marine Environmental Laboratory Contribution Number 2207.

Corresponding author address: William S. Kessler, NOAA/PMEL/OC, 7600 Sand Point Way NE, Seattle, WA 98115.
E-mail: kessler@pmel.noaa.gov

has the advantage that it consistently identifies an intraseasonal signal that can be described as tropically trapped, with largest amplitude over the Indian and west Pacific Oceans, and eastward propagating, with low zonal wavenumber and speeds of a few meters per second. Other indices for interannual MJO activity tend to be correlated with those derived from the largest EOFs. For example, Slingo et al. (1999) compared several measures and recommended the zonal mean of bandpassed 200-mb zonal wind as the simplest index; Hendon et al. (1999) found a correlation of 0.78 between this and several other interannual EOF indices.

The conundrum for those wishing to understand the relation between the MJO and the onset of El Niño is that, on the one hand, recent El Niños have seen a tantalizing set of prominent intraseasonal events (Kessler et al. 1995; McPhaden and Yu 1999), but, on the other hand, the interannual MJO activity time series that emerge from an EOF decomposition or from the zonal average measures are uncorrelated with the Southern Oscillation index (SOI) or other indices of the ENSO cycle (Slingo et al. 1999). Since the EOF indices are so widely used and accepted as a convenient way to represent MJO activity, it seems worthwhile to look into what aspects of the MJO are depicted by this method and to try to resolve the apparent discrepancy between these indices and the often-remarked occurrence of strong intraseasonal variability during recent El Niño events.

In examining a possible MJO–ENSO connection, it is the Pacific that is important, and relatively small zonal shifts of MJO activity over the western Pacific can make a large proportional difference in its effects on the ocean. Therefore, it is of great interest, first, whether intraseasonal activity does in fact move east and west interannually and, second, whether such meandering encompasses the MJO. The reason for making a distinction between the MJO and intraseasonal activity in general is not just semantic. The MJO is a unified, global-scale physical phenomenon whose dynamics and thermodynamics and interaction with the underlying ocean can be studied and understood and perhaps someday predicted (or at least its statistical properties may be predictable). The utility of EOF analysis in this context is that it extracts the coherent large-scale signal and thus allows one to distinguish between intraseasonal variance of unspecified origin and that due to the MJO.

Section 2 describes the data used here and their treatment. Section 3 gives results, and section 4 discusses the implications for the ENSO cycle.

2. Data and processing

a. Outgoing longwave radiation

Pentad averages of twice-daily OLR observed by satellite are used in this study to estimate the location and strength of tropical deep convection (Rui and Wang 1990). This dataset has been the basis for numerous studies of tropical convective activity in which low values of OLR indicate the presence of tall cumulus towers associated with intense convection (Waliser et al. 1993). The global observations are binned into a 2.5° by 2.5° global grid. Here we use the unbroken 1979–99 time series in the global tropical strip, averaged over 5°S–5°N.

b. Operational zonal wind

European Centre for Medium-Range Weather Forecasts (ECMWF) operational twice-daily 10-m zonal wind for the period of 1985–99 was used as a check on the OLR results. All the analyses done with OLR were carried out identically with zonal wind, and some findings are cited below. I chose to work principally with OLR since the results were generally similar and the OLR time series is about 40% longer. Hendon et al. (1999) also found parallel results analyzing MJO indices based on OLR and 850-mb zonal wind. A further disadvantage of the zonal wind time series for present purposes is that its variance tends to be dominated by the extreme anomalies during the 1997–98 El Niño, which is less true for OLR.

c. Bandpass filtering

Both the OLR and zonal wind time series were bandpass filtered with a Lanczos filter with 49 weights and half-power frequency cutoffs of 20 and 90 days^{-1} (Jones et al. 1998; Duchon 1979). Although similar results were found using a cruder bandpass, the advantage of the Lanczos filter is that it preserves almost all of the variance within its window [see Fig. A1 of Jones et al. (1998)].

d. Interannual variability of intraseasonal time series

A measure of the interannual signature of the various intraseasonal time series discussed here is constructed by squaring the bandpassed data, smoothing the squares with a 1-yr running mean, and then taking the square root. This quantity, which has the same units as the original data, will be referred to as the ''interannual amplitude'' of the intraseasonal quantity in question. For example, Fig. 1 shows the interannual amplitude of intraseasonal OLR.

e. Significance of correlations

Significance of correlations cited here was estimated through the procedure in Kessler et al. (1996), based on estimating the degrees of freedom from the independence timescale of Davis (1976). Correlations r are cited only if they are significantly different from zero at the 95% level. Typically, correlations among the 20-yr interannual amplitude time series studied here were found

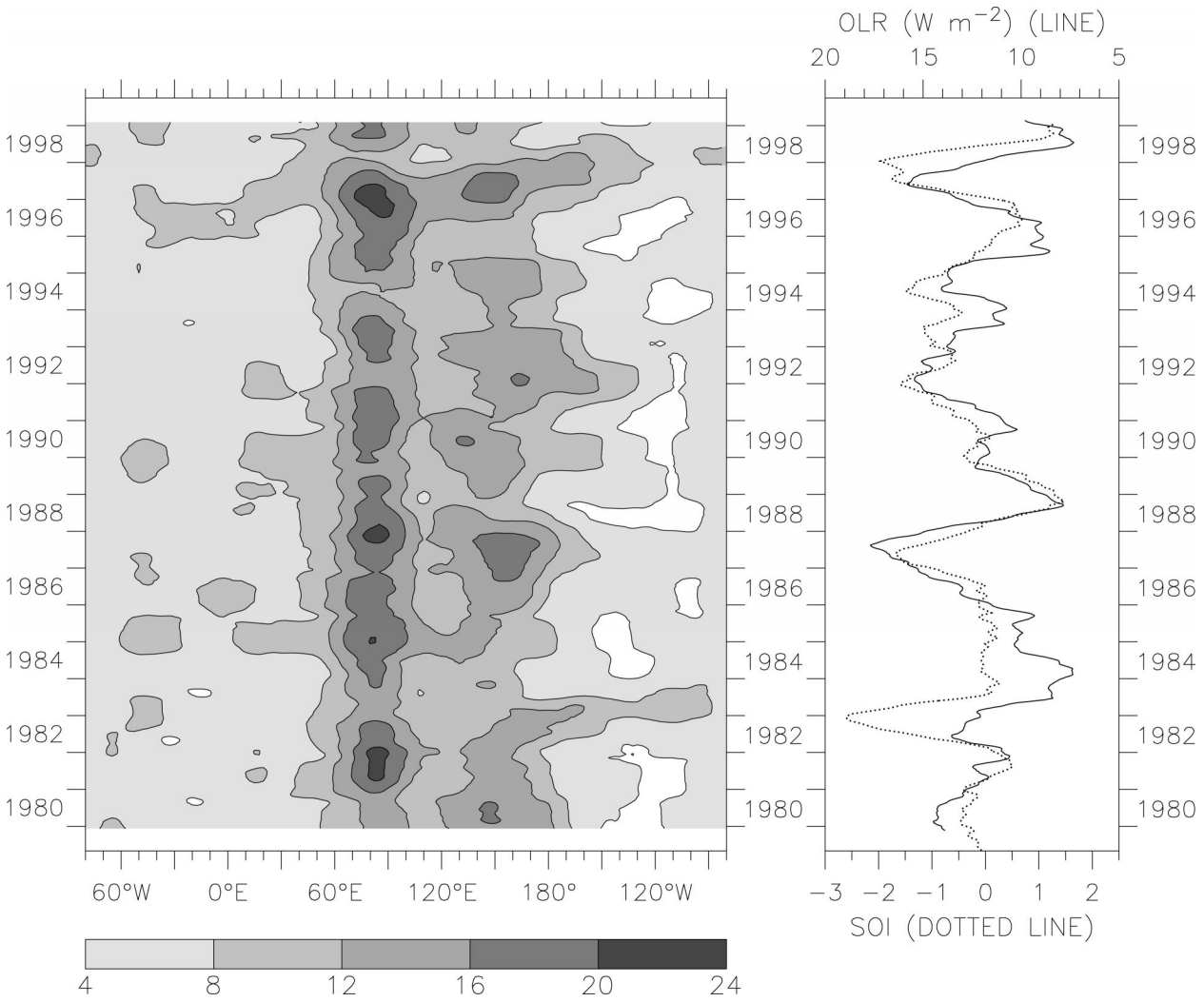

FIG. 1. Interannual amplitude of intraseasonal OLR (5°S–5°N) (W m^{-2}) (see section 2d for definition). (left) Amplitude in the global tropical strip, centered on the major region of variance (the abscissa extends around the globe, broken at the South American coast at 80°W). (right) time series of OLR interannual amplitude averaged over the western Pacific (150°E–180°) (solid line, scale at top) in comparison with the SOI (dotted line, scale at bottom). Year ticks on each panel are at 1 Jan of each year, with year labels centered at midyear.

to have 20–30 degrees of freedom according to the Davis timescale, implying that correlations with absolute values larger than about 0.45 were significantly different from zero.

f. Significance of EOFs

The term principal component (PC) is used here to refer to the temporal eigenvectors of the EOF decomposition. The EOFs are normalized to place the dimensions of the data in the spatial eigenvectors, with the PCs being nondimensional. Significance of EOF modes was estimated by the North et al. (1982) criteria, based on comparing the separation between neighboring eigenvalues with an estimate of the sampling error. For this measure, the degrees of freedom in the PCs were taken to be the number of pentads in the time series divided by the typical intraseasonal period (8 pentads). Only EOFs that clearly exceed the North et al. criteria are discussed.

g. The Southern Oscillation index

The SOI is the monthly average sea level pressure difference between Tahiti and Darwin, Australia, demeaned and normalized by its standard deviation (Chelliah 1990). Negative values of the SOI occur during El Niños, positive values during La Niñas. The time series used here were prepared by the National Centers for Environmental Prediction. For comparison with the interannual amplitude of the intraseasonal variables, the SOI was smoothed with a 1-yr running mean.

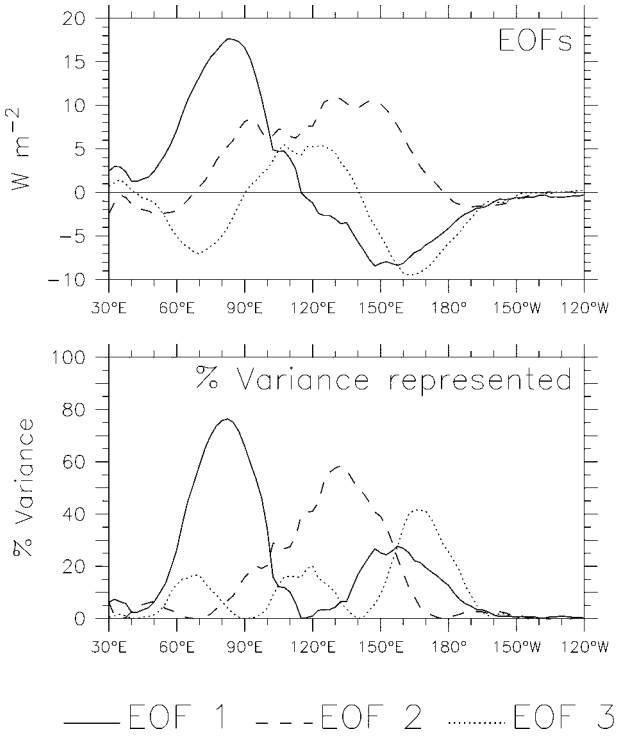

FIG. 2. Spatial patterns of EOFs 1–3 of intraseasonal OLR. (top) EOF spatial patterns (W m^{-2}). (bottom) Percent variance at each location represented by the three EOFs. Although the EOFs are calculated around the global tropical strip, only the Indo-Pacific region 30°E–120°W is shown, since the EOFs are near zero elsewhere.

3. Results

Intraseasonal variability of OLR has its main center near 90°E in the eastern Indian Ocean, with a minimum over the ''Maritime Continent'' near 120°E and a second (weaker) maximum over the western Pacific between about 140°E and the date line (Fig. 1, left). As is evident from Fig. 1, the Pacific maximum fluctuates differently than the main center over the Indian Ocean: the correlation of interannual OLR amplitude at 90°E with this amplitude in the rest of the tropical strip falls sharply to zero by 165°E. Although the Indian Ocean region is uncorrelated with the SOI, interannual amplitude of OLR over the western Pacific is closely related to the ENSO cycle (Fig. 1, right), with larger amplitude during El Niño events ($r = -0.62$). OLR intraseasonal variability extends eastward during El Niño events (as well as at a few other times, discussed below). It is this regular association of enhanced intraseasonal activity over the west Pacific during El Niño (also seen in zonal winds) that has stirred interest in a possible MJO–ENSO connection.

An EOF decomposition of bandpassed OLR produces a quadrature pair of modes similar to those found by other authors, as well as at least one other significant mode (Fig. 2, top). EOF 1 has out-of-phase maxima in the eastern Indian Ocean and the west Pacific, and EOF 2 has one maximum between these two peaks. The PCs for modes 1 and 2 are highly lag correlated ($r > 0.5$), with PC 1 leading PC 2 by 10–15 days, demonstrating the familiar eastward-propagating intraseasonal oscillation from about 60° to 160°E, decaying to the east.

Indices of MJO activity can be made from the low-passed time series of the variance of PC 1 (Slingo et al. 1999) or from a linear combination of PCs 1 and 2 (Maloney and Hartmann 1998; Jones 2000) or from the global average variance reconstructed from EOFs 1 and 2 (Hendon et al. 1999). Interannual variability of such indices has been found to be uncorrelated with measures of the ENSO cycle (Hendon et al. 1999; Slingo et al. 1999), and the same is found here from the first two EOFs shown in Fig. 2, with $r \approx 0$ between the SOI and all these kinds of indices constructed from the current data for the period of 1979–99. If anything, there is a suggestion that the MJO is less active in its main Indian Ocean region during the height of warm events (especially during 1983 and 1998; Fig. 1).

The third EOF of intraseasonal OLR (Fig. 2) has not previously been considered in the literature. The first two EOFs combined represent about 40% of the total variance of intraseasonal OLR in the global equatorial strip; EOF 3 represents only 9.2% overall. Nevertheless, it stands well above the North et al. (1982) rejection criteria by a factor of about 3. Its maximum is found in the region of 150°E–170°W, in the west Pacific warm pool where mechanisms proposed for MJO–ENSO interaction occur (e.g., Kessler and Kleeman 2000). EOF 3 represents over 40% of the total variance between 160° and 170°E, where it is dominant (Fig. 2, bottom), suggesting that, if it can be shown to portray an aspect of the MJO not depicted by the usual first mode pair, then it may add a meaningful piece of the puzzle.

The spatial pattern of EOF 3, with one positive and two negative lobes, probably does not represent a discrete physical process on its own (Fig. 2, top). This structure may be forced by the requirement for orthogonality of the EOFs, resulting in one spatial pattern with no zero crossings, one with one, one with two, and so on. This apparently unphysical property of the EOF solution may be why previous investigators have not looked past the first mode pair. By itself, the interannual amplitude of PC 3 is only weakly correlated with the SOI ($r = -0.34$, which is not significant at the 95% level). Instead, its importance occurs because of its phasing relative to EOF 1. By definition, PCs 1 and 3 are uncorrelated when the correlation is taken over all time, but this is not necessarily true for any partial time range. The correlation (at zero lag) between PCs 1 and 3 was calculated within a running 400-day window. This running correlation is shown in Fig. 3, in which it is compared with the SOI. The correlation averages to zero over the full 20-yr record, but its temporal structure is itself well correlated with the SOI ($r = -0.68$), as is obvious in Fig. 3. Positive correlation between PCs 1 and 3 occurs during El Niño events. During these periods, PCs 1 and 3 have the same sign, so EOFs 1 and

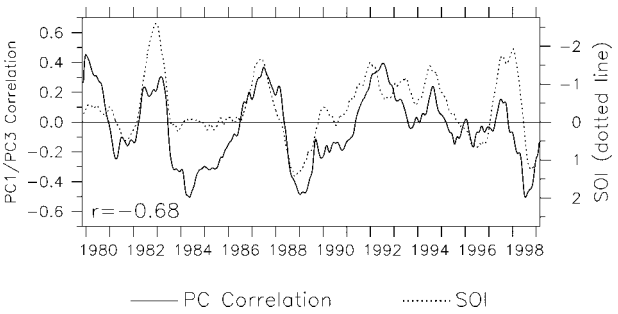

FIG. 3. Running correlation between PCs 1 and 3 of OLR (solid line, scale at left) in comparison with the SOI (dotted line, scale at right, inverted so El Niños are up on the plot). The correlation is calculated in a running 400-day window for the 20-yr time series. The correlation between the two time series shown here is −0.68 as noted in the label.

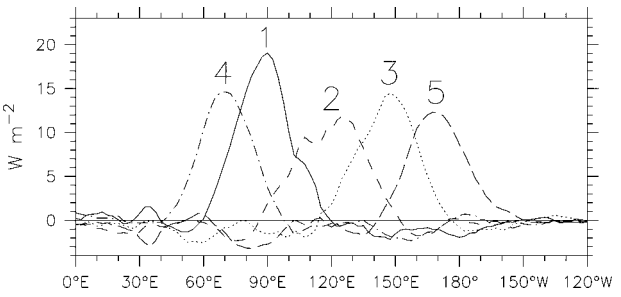

FIG. 4. Spatial patterns of the first five rotated EOFs of intraseasonal OLR (W m^{-2}). Numbers above each peak indicate the REOF number as referred to in the text. The calculation was performed over the global tropical strip, but only the Indo-Pacific region 0°–120°W is shown here since the EOFs are near zero elsewhere.

3 take the relative structures shown in Fig. 2 (top), and EOF 3 weakens EOF 1 in the Indian Ocean and strengthens EOF 1 in the Pacific, thereby extending the MJO envelope to the east. When the correlation is negative (during La Niña and neutral periods, Fig. 3), EOF 3 reduces the eastward extent of MJO propagation into the Pacific by weakening EOF 1 there. This well-organized phasing of EOF 3 suggests that a more complete description of the MJO would include the first three EOFs combined, showing the coherent eastward-propagating signal meandering east and west interannually with the ENSO cycle. A similar conclusion is equally apparent in the parallel analysis based on zonal winds.

This impression is strengthened by rotating the EOFs to simplify the patterns represented. Rotated EOFs (REOFs) are especially useful when the physical interpretation of the unrotated EOFs appears to be muddied by artificially geometric patterns forced by the spatial orthogonality constraint [Richman (1986); see Horel (1981) for a particularly lucid discussion]. Maximizing the sum of fourth powers of the eigenvectors (rather than their squares as in the EOF solution) causes the spatial patterns to have a few, usually separate, maxima rather than the overlapping, partially cancelling patterns seen in the ordinary EOFs (e.g., Fig. 2, top). These are often more easily associated with physical phenomena (but of course there is no guarantee that the rotated EOFs will be physical modes). Although there are objective criteria for choosing the number of EOFs to rotate (Preisendorfer et al. 1981), others have found that the results are relatively insensitive to the choice within a fairly wide range (Horel 1981), and by experiment I settled on rotating 10 EOFs by the varimax method (rotating more EOFs made only slight changes in the nature of the resulting modes).

The first five REOF spatial patterns line up as a series of peaks from west to east with about the same zonal extent as the original three EOFs (Fig. 4). REOF 1 is centered at the main maximum of intraseasonal activity (Fig. 1) and represents about 17% of the total variance; the other four represent about 10% each. These five REOFs are well separated from the higher rotated modes whose amplitude drops off by a factor of 2. The PC of each successive peak is significantly correlated with the peak to its east with a lead of 10–15 days, representing an eastward speed of about 3 m s^{-1} (slightly faster across the Maritime Continent and slightly slower across the open-ocean regions of both the Indian and Pacific). Most important for current purposes is the interannual variation of the rotated PC time series. Interannual amplitude of the western three rotated PCs is uncorrelated with the SOI, but that of the easternmost PC (5) is negatively correlated with the SOI ($r = -0.69$; that is, it is stronger during El Niños). Rotated PC 3 (representing the far western Pacific) is weakly negatively correlated with the SOI, and inspection of the time series shows some periods in which it varies with the SOI and some in which it does not. The five REOFs together show intraseasonal MJO events propagating eastward across the Indian Ocean and Maritime Continent with interannual variations largely unrelated to ENSO, but during El Niños the pattern extends eastward, and during La Niñas, it retreats westward.

4. Discussion

An EOF decomposition of intraseasonally bandpassed OLR around the tropical strip identified two kinds of coherent interannual variability. First, the overall activity of the MJO, represented either by the first two simple EOFs or the first four rotated EOFs, is uncorrelated with the ENSO cycle. This signal shows the activity of the MJO in its central region and is similar to results that have been noted by several investigators (Slingo et al. 1999; Hendon et al. 1999). Second, the third simple EOF or the fifth rotated EOF combine with the lower modes to demonstrate an east–west meandering of the MJO envelope that is clearly associated with ENSO. Both kinds of EOF representation show intraseasonal oscillations propagating eastward from the Indian to the western Pacific Ocean, with propagation extending about 20° of longitude farther east during El Niño events. A very similar set of EOFs was found for 10-m

zonal wind from the ECMWF analysis. The fact that the eastward shift is seen in the low-mode, spatially coherent EOFs that have well-defined and consistent intraseasonal phase relationships among them shows that both modes of variability make up the interannual signature of the MJO and are not just enhanced, but incoherent, convective activity over the Pacific during El Niño.

The first five REOFs together represent about 55% of total OLR intraseasonal variance, which can be considered as the MJO part. If we take REOFs 1–4 as representing the overall MJO activity and REOF 5 as its eastward extension, then about 80% of the MJO variance is associated with fluctuations of overall activity and 20% with the zonal shift.

The eastward extension is important because it means that ENSO-related MJO activity occurs over the west Pacific warm pool, for which recent work has pointed to rectifying mechanisms that can couple the MJO to the development of El Niño events (Kessler and Kleeman 2000). The average eastern edge of the MJO envelope occurs over the far western Pacific (close to the coast of New Guinea), but relatively small zonal shifts can produce large proportional changes in the fetch of MJO winds over the Pacific, bringing them out over the open ocean where SST changes can be driven by equatorial processes. However, there is no suggestion of the MJO leading El Niño. It is likely that the expanding MJO is a consequence, not a cause, of the warming west-central Pacific, in which warm SST allows the convection to spread eastward (Fink and Speth 1997). However, once the eastward expansion occurs, it then allows MJO–ENSO interaction over the Pacific to influence the evolution of the event.

The zonal shift of the MJO also has implications for the development of models of the ocean–atmosphere feedbacks that characterize the ENSO cycle. These feedbacks depend on the relative position of the winds to the interannually varying SST. Air–sea exchanges evaluated from a fixed-position MJO composite cannot adequately address such feedbacks, so it is essential to take the interannual changes in the width of the MJO envelope into account.

It is also worth noting that there were two other occasions on which enhanced MJO activity was seen over the far western Pacific, in 1979–80 and, to a lesser degree, in 1989–90 (Fig. 1). Both were periods during which the SOI turned negative but full-blown El Niños did not develop. Donguy and Dessier (1983) described El Niño–like changes in the west Pacific during 1979–80, noting especially low salinity anomalies suggestive of increased precipitation and weakened westward advection. Although it apparently was not described in the literature, at the time there was much speculation that conditions during 1989 were setting up a warm event (B. Kessler 2000, personal communication). SST in the equatorial Pacific west of 150°W grew 0.5°–1°C anomalously warmer during 1989, so this may have been comparable to a pre-Niño period. In both cases, although El Niño events did not develop, the west Pacific apparently was sufficiently El Niño–like that the MJO envelope did extend east.

The purpose of this note is to make the simple point that it is not the zonal average or total MJO activity that is related to ENSO, but a specific element of it, namely, the meandering that moves the intraseasonal winds over the Pacific where SST is very sensitive to equatorial ocean processes. Global activity indices of interannual fluctuations of the MJO necessarily focus substantial weight on the Indian Ocean region that is not the aspect most important to ENSO. The zonal shift is not associated with large changes in the global activity, so the traditional activity indices are not especially relevant when considering mechanisms by which the MJO and the ENSO cycle might interact. It is unfortunate that no simple index of the MJO relation to ENSO emerges from this study. However, the MJO–ENSO association is unambiguous, with each of the El Niño events since 1979 clearly associated with an eastward extension of the MJO envelope, and the La Niña periods with a westward retreat. This suggests that a complete understanding of the evolution of the ENSO cycle depends on understanding the role of the MJO in it, and the question will not be represented as a simple change in global MJO activity.

Acknowledgments. The author thanks Dennis Hartmann, Harry Hendon, Mike McPhaden, Dennis Moore, and Mike Wallace for illuminating discussions and many helpful suggestions. I also thank several colleagues whose vigorous response to earlier papers on this subject, in which they pointed out the lack of correlation of MJO indices with the ENSO cycle, inspired me to figure out where the discrepancy lay. ECMWF kindly allowed use of their operational winds. Support for this work came from NOAA's Office of Global Programs through the Stanley P. Hayes Center.

REFERENCES

Chelliah, M., 1990: The global climate for June–August 1989: A season of near-normal conditions in the tropical Pacific. *J. Climate*, **3,** 138–160.

Davis, R. E., 1976: Predictability of sea surface temperature and sea level pressure anomalies over the North Pacific Ocean. *J. Phys. Oceanogr.,* **6,** 249–266.

Donguy, J.-R., and A. Dessier, 1983: El Niño-like events observed in the tropical Pacific. *Mon. Wea. Rev.,* **111,** 2136–2139.

Duchon, C. E., 1979: Lanczos filtering in one and two dimensions. *J. Appl. Meteor.,* **18,** 1016–1022.

Fink, A., and P. Speth, 1997: Some potential forcing mechanisms of the year-to-year variability of the tropical convection and its intraseasonal (25–70-day) variability. *Int. J. Climatol.,* **17,** 1513–1534.

Gutzler, D. S., 1991: Interannual fluctuations of intraseasonal variance of near-equatorial zonal winds. *J. Geophys. Res.,* **96,** 3173–3185.

Hendon, H. H., C. Zhang, and J. D. Glick, 1999: Interannual variability of the Madden–Julian oscillation during austral summer. *J. Climate,* **12,** 2538–2550.

Horel, J. D., 1981: A rotated principal component analysis of the interannual variability of the Northern Hemisphere 500 mb height field. *Mon. Wea. Rev.,* **109,** 2080–2092.

Jones, C., 2000: Occurrence of extreme precipitation events in California and relationships with the Madden–Julian oscillation. *J. Climate,* **13,** 3576–3587.

——, D. E. Waliser, and C. Gautier, 1998: The influence of the Madden–Julian oscillation on ocean surface heat fluxes and sea surface temperature. *J. Climate,* **11,** 1057–1072.

Kessler, W. S., and M. J. McPhaden, 1995: Oceanic equatorial waves and the 1991–93 El Niño. *J. Climate,* **8,** 1757–1774.

——, and R. Kleeman, 2000: Rectification of the Madden–Julian oscillation into the ENSO cycle. *J. Climate,* **13,** 3560–3575.

——, M. J. McPhaden, and K. M. Weickmann, 1995: Forcing of intraseasonal Kelvin waves in the equatorial Pacific. *J. Geophys. Res.,* **100,** 10 613–10 631.

——, M. C. Spillane, M. J. McPhaden, and D. E. Harrison, 1996: Scales of variability in the equatorial Pacific inferred from the TAO buoy array. *J. Climate,* **9,** 2999–3024.

Lau, K.-M., and P. H. Chan, 1988: Intraseasonal and interannual variations of tropical convection: A possible link between the 40–50 day oscillation and ENSO? *J. Atmos. Sci.,* **45,** 506–521.

Luther, D. S., D. E. Harrison, and R. A. Knox, 1983: Zonal winds in the central equatorial Pacific and El Niño. *Science,* **222,** 327–330.

Madden, R. A., and P. A. Julian, 1994: Observations of the 40–50-day tropical oscillation—a review. *Mon. Wea. Rev.,* **122,** 814–837.

Maloney, E. D., and D. L. Hartmann, 1998: Frictional moisture convergence in a composite life cycle of the Madden–Julian oscillation. *J. Climate,* **11,** 2387–2403.

McPhaden, M. J., 1999: Genesis and evolution of the 1997–98 El Niño. *Science,* **283,** 950–954.

——, and X. Yu, 1999: Equatorial waves and the 1997–98 El Niño. *Geophys. Res. Lett.,* **26,** 2961–2964.

Moore, A. M., and R. Kleeman, 1999: Stochastic forcing of ENSO by the intraseasonal oscillation. *J. Climate,* **12,** 1199–1220.

North, G. R., T. L. Bell, R. F. Cahalan, and F. J. Moenig, 1982: Sampling errors in the estimation of empirical orthogonal functions. *Mon. Wea. Rev.,* **110,** 669–706.

Preisendorfer, R. W., F. W. Zwiers, and T. P. Barnett, 1981: Foundations of principal coordinate selection rules. SOI Reference Series 81-4, Scripps Institution of Oceanography, La Jolla, CA, 192 pp.

Richman, M. B., 1986: Rotation of principal components. *J. Climatol.,* **6,** 293–335.

Rui, H., and B. Wang, 1990: Development characteristics and dynamic structure of tropical intraseasonal convection anomalies. *J. Atmos. Sci.,* **47,** 357–379.

Shinoda, T., H. H. Hendon, and J. Glick, 1998: Intraseasonal variability of surface fluxes and sea surface temperature in the tropical western Pacific and Indian Oceans. *J. Climate,* **11,** 1685–1702.

Slingo, J. M., D. P. Rowell, K. R. Sperber, and F. Nortley, 1999: On the predictability of the inter annual behavior of the Madden–Julian oscillation and its relationship with El Niño. *Quart. J. Roy. Meteor. Soc.,* **125,** 583–609.

Verbickas, S., 1998: Westerly wind bursts in the tropical Pacific. *Weather,* **53,** 282–284.

Waliser, D. E., N. E. Graham, and C. Gautier, 1993: Comparison of highly reflective cloud and outgoing longwave radiation datasets for use in estimating tropical convection. *J. Climate,* **6,** 331–353.

Weickmann, K. M., 1991: El Niño/Southern Oscillation and Madden–Julian (30–60 day) oscillations during 1981–82. *J. Geophys. Res.,* **96,** 3187–3195.

Zhang, C., and H. H. Hendon, 1997: Propagating and standing components of the intraseasonal oscillation in tropical convection. *J. Atmos. Sci.,* **54,** 741–752.